Journal of Asian Multicultural Research for Medical and Health Science Study
ISSN: 2708-972X
Vol. 7, No. 1, 2026 (page 001-010)
DOI: https://doi.org/10.47616/jamrmhss.v7i1.682

Identification and Comparison of Functional Groups in Medicinal plants using Attenuated Total Reflectance–Fourier Transform Infrared (ATR-FTIR) Spectroscopy

Komal Kumar Javarappa[1], Adarsh Panchakshari[1], Sankeerthana Renukaprasad[1], Mallikarjunaswamy Pramod[1]

[1]University Sophisticated Instrumentation Centre (USIC), JSS Academy of Higher Education and Research (JSS AHER), Mysuru, Karnataka, India
Email: komalkumar@jssuni.edu.in

Received: December 15, 2025 Received in Revised: January 30, 2026 Accepted: March 17, 2026

Abstract

The biochemical profiles of a few chosen medicinal plant leaves in both fresh and shade-dried forms were examined and compared using attenuated total reflectance–Fourier transform infrared (ATR-FTIR) spectroscopy. Major functional groups were to be identified, spectral variations across treatment conditions were assessed, and the impact of drying on spectral clarity was to be ascertained. Samples were scanned in the mid-infrared range (4000–400 cm^{-1}), and spectra were generated using baseline correction, normalization, and averaging among repeats. Prominent bands of absorption that correspond to O–H stretching (~3300 cm^{-1}), C–H stretching of aliphatic groups (2920–2850 cm^{-1}), C=O and C=C vibrations of phenolic and flavonoid compounds (~1700–1600 cm^{-1}), and carbohydrate-related C–O–C and C–O stretching (1100–1000 cm^{-1}) have been consistently identified across species. Fresh samples displayed wide and powerful O–H bands due to greater moisture content, which concealed underlying biomolecular characteristics. Shade-drying considerably decreased water-associated absorptions, increasing the resolution of protein (amide I and amide II), lipid, and polysaccharide bands. Interspecific differences in band intensities were found through comparative analysis, suggesting variations in the composition of phytochemicals like phenolics, alkaloids, terpenoids, and glycosides. ATR-FTIR is a quick, non-destructive analytical method that can produce repeatable biochemical fingerprints for therapeutic plants. Shade-dried leaves were shown to provide sharper spectral fingerprints than fresh material, indicating their applicability for spectroscopic authentication and phytochemical screening. These findings provide baseline FTIR spectrum assignments for the investigated species and show the potential of vibrational spectroscopy for quality control.

Keywords: ATR-FTIR, Functional Groups, Medicinal Plants, Biomolecules, Phytochemicals

Introduction

Medicinal plants have long been central to traditional folk medicine, forming a key component of traditional ecological knowledge. For centuries, ancient civilizations have relied on these plants for their therapeutic properties and healing effects, and this knowledge has been preserved and passed down through generations (Süntar, 2020). Medicinal plants continue to play a vital role in the management of numerous diseases, largely due to the diverse secondary metabolites they produce. These metabolites commonly referred to as bioactive compounds are responsible for the plants curative potential and are of significant interest in modern drug discovery (Xiong & Long, 2020; Lowe et al., 2021).

Bioactive compounds exhibit a broad spectrum of pharmacological activities, including antimicrobial, antioxidant, anti-inflammatory, and anticancer effects, making them valuable candidates for therapeutic development (Tran et al., 2020). Identifying and characterizing these compounds is essential for understanding the medicinal potential of plant species, as they offer promising avenues for the treatment of chronic, acute, and infectious diseases (Fu et al., 2019).

Increasing attention has been directed toward medicinal plants that contain exceptionally high levels of antioxidants, phenolics, diterpenoids, and alkaloids (Süntar, 2020; Xiong & Long, 2020). These classes of compounds are widely recognized for their diverse pharmacological properties, particularly their cardiovascular and general health benefits [3–5]. Several of these plants hold significant potential for human use, either as medicinal resources or as functional foods due to their bioactive profiles (Moussaoui & Alaoui, 2016).

Beyond their direct therapeutic value, many medicinal plants are utilized in a variety of applications. They serve as traditional medicines (Zengin et al., 2018; Subash et al., 2015; Shahidi & Ambigaipalan, 2015; Cai et al., 2004) , as sources of animal fodder, as natural food additives that delay oxidative processes (Lee et al., 2003; Dal Bosco et al., 2019), and as reducing agents in the synthesis of nanomaterials (Vuong et al., 2014). Their richness in natural antioxidants further enhances their utility across multiple fields, underscoring their importance as versatile biological resources with broad scientific and industrial relevance (Blonk & Cock, 2019; Aziza et al., 2010)

Understanding the molecular fingerprint of medicinal plants is essential for identifying the bioactive compounds responsible for their therapeutic effects. These plants contain diverse phytochemicals, many of which can be targeted for the treatment of specific diseases. Therefore, dissecting and characterizing the biochemical signatures of medicinal plants is a critical step in advancing their pharmacological applications (Sytar et al., 2018)

Among the various analytical tools available, Fourier Transform Infrared (FTIR) spectroscopy is one of the most widely used and powerful techniques for profiling plant molecular fingerprints. FTIR provides valuable insight into the functional groups and chemical constituents present in plant tissues, making it a crucial method for elucidating the biochemical composition of medicinal species (Mandrone et al., 2019; Walters et al., 2019)

Researchers have utilized FTIR spectroscopy to examine the biomolecular composition of several medicinal plant species, including *Atylosia albicans*, *Tephrosia tinctoria*, *Humboldtia brunonis*, *Kingiodendron pinnatum*, *Derris scandens*, and *Caesalpinia mimosoides*. These analyses reveal that the plants are rich in phenolic compounds and also contain notable levels of oligosaccharides, phosphates, proteins, carbohydrates, carotenoids, lignin, and polysaccharides. The findings clearly highlight distinct variations in the categories of chemical constituents among the taxa studied.

Moreover, the distribution and concentration of these biomolecules differ across various plant parts, underscoring the biochemical diversity within and between species (Maaloul et al., 2024) (Kumar & Devi Prasad, 2011). In this context, we aimed to characterize and compare the molecular fingerprints of these plant leaves before and after drying using ATR-FTIR spectroscopy.

Methods

Collection and Identification of Plant Material

Leaves from five medicinal plants guava (*Psidium guajava*), amla (*Phyllanthus emblica*), papaya (*Carica papaya*), neem (*Azadirachta indica*), and Ashanti Blood (*Mussaenda*

erythrophylla were collected from the Herbal Garden of JSS College of Pharmacy, Mysuru District, Karnataka, India. Fresh, healthy leaves were excised, cleaned thoroughly, and powdered using a sterile pestle and mortar.

Preparation of Plant Material Powder

To compare the functional group profiles of fresh and dried samples, the collected leaves were divided into two sets. Fresh leaves were powdered immediately after cleaning. For dried samples, leaves were shade dried at room temperature in a clean environment for seven days to prevent contamination, and then finely powdered using a pestle and mortar. All powdered samples were stored in airtight containers and analysed immediately using ATR-FTIR to avoid moisture interference.

Spectroscopic Analysis

ATR-FTIR spectra were recorded using a PerkinElmer spectrometer. Both fresh and shade-dried powdered samples were scanned at room temperature (25 ± 2 °C) over a spectral range of 4000–400 cm^{-1} with 16 scans per sample. To enhance the signal-to-noise ratio, 100 interferograms were averaged at a spectral resolution of ±4 cm^{-1}. Background spectra, obtained under identical conditions, were automatically subtracted from the sample spectra. Each sample was analysed in five replicate powder preparations, with careful attention to consistency in powdering. This standardized approach ensured that the absorption band intensities could be directly correlated with the concentrations of the corresponding functional groups (Lowe et al., 2021).

Table 1. FTIR Spectral Regions and Corresponding Functional Groups with Indicated Phytochemicals

Peak Region (cm^{-1})	Functional Group	Phytochemicals Indicated	Reference
3600–3200	O–H stretching	Phenols, polyphenols, flavonoids, tannins	Movasaghi et al., 2008
3300–3200	N–H stretching	Alkaloids, amino compounds	Cordero Otero et al., 2003
3000–2800	Aliphatic C–H stretching	Terpenoids, fatty acids, lipids	Quero et al., 2025
1760–1680	C=O stretching	Organic acids, esters, flavonoids	Wongsa et al., 2022a
1650–1600	Aromatic C=C / Amide I	Flavonoids, phenolics, proteins	Ji et al., 2020
1580–1500	Amide II (N–H bending)	Protein components	Tauchen et al., 2020
1500–1450	Aromatic C=C	Flavonoids, tannins	Shin et al., 2015
1450–1370	CH_2 / CH_3 bending	Terpenoids, lipids	Khakhalary & Narzari, 2025
1350–1300	C–N stretching	Alkaloids, proteins	El Orche et al., 2024
1300–1000	C–O and C–O–C stretching	Phenols, flavonoids, carbohydrates	Higgixs et al., 1961
1100–1000	Glycosidic C–O–C	Polysaccharides	Pan et al., 2007
900–690	Aromatic C–H (out-of-plane)	Aromatic phenolics, flavonoids	Kancherla et al., 2025a

600–400	Fingerprint region	Mixed phytochemicals	Umar et al., 2023

Table 2. FTIR Peak Assignments of Selected Medicinal Plants

Plant Name	Peak (cm^{-1})	Functional Group Assignment	Reference
Ashanti Blood	3338	O–H / N–H stretching	Janakiraman & Johnson, 2015
Ashanti Blood	2924	C–H stretching	Ebrahimi & Parvinzadeh Gashti, 2016
Ashanti Blood	1634	Amide I / Aromatic C=C	El Orche et al., 2024
Ashanti Blood	1377	CH_2 bending	Priya & Asharani, 2018
Ashanti Blood	1049	C–O stretching	Yahaya et al., 2023
Ashanti Blood	3288	O–H stretching	Wongsa et al., 2022b
Ashanti Blood	2918	C–H stretching	Pharmawati & Wrasiati, 2020
Ashanti Blood	1615	Amide I / Aromatic C=C	Thomaspaulraj et al., 2014
Ashanti Blood	1318	C–N stretching	Cintrón & Hinchliffe, 2015
Ashanti Blood	1027	C–O stretching	Mekonnen, 2023
Neem	3289	O–H stretching	P. Zhang et al., 2024
Neem	2921	C–H stretching	Kamnev et al., 2023
Neem	1635	Amide I	Shi et al., 2012
Neem	1543	Amide II	Quero et al., 2025
Neem	1034	C–O stretching	Senthilkumar & Sivakumar
Neem	3287	O–H stretching	Agatonovic-Kustrin et al., 2021
Neem	2920	C–H stretching	Christou et al., 2018
Neem	1606	Aromatic C=C	Dimakopoulou-Papazoglou et al., 2025
Neem	1245	C–O stretching	Y. C. Zhang et al., 2022
Amla	3293	O–H stretching	Chiang et al., 2023
Amla	2920	C–H stretching	J et al., 2024
Amla	1631	Amide I	Pasieczna-Patkowska et al., 2025
Amla	1443	CH_2 bending	Thombare et al., 2023
Amla	1037	C–O stretching	Bouyanfif et al., 2019
Amla	3287	O–H stretching	Capobianco et al., 2023
Amla	1632	Amide I	Kalisz et al., 2021
Amla	1240	C–O stretching	—
Guava	3335	O–H stretching	Tew et al., 2022
Guava	2918	C–H stretching	Tasleem et al., 2019
Guava	1634	Aromatic C=C	Dev & Mukadam, 2025
Guava	1046	C–O stretching	Cruz-Espinoza et al.
Guava	3289	O–H stretching	Krysa et al., 2022

Guava	2919	C–H stretching	Fontes et al., 2022
Guava	1615	Aromatic C=C	Dev & Mukadam, 2025
Guava	1024	C–O stretching	Ayvaz & Temizkan, 2018
Papaya	3288	O–H stretching	Cintrón & Hinchliffe, 2015
Papaya	2919	C–H stretching	Rasli et al., 2020
Papaya	1635	Amide I	A et al.
Papaya	1052	C–O stretching	Pasieczna-Patkowska et al., 2025
Papaya	3279	O–H stretching	Fadzil & Othman, 2024
Papaya	2921	C–H stretching	Thomaspaulraj et al., 2014
Papaya	1633	Amide I	Kancherla et al., 2025b
Papaya	1048	C–O stretching	Fontes et al., 2022

Results and Discussion

The basic tenet of FT-IR relies on vibration of chemical bonds in the IR region. In the IR region, chemical bonds absorb radiation between 4000 and 400 cm1. In this study, ATR-FTIR profiling of both fresh and dried leaves from 5 different plants was performed to see any comparative changes before and after draying. All the samples were scanned from 400-4000cm-1 wave number (Nikalje et al., 2019).

The representative ATR- FTIR spectra Leaves from five medicinal plants guava (*Psidium guajava*), amla (*Phyllanthus emblica*), papaya (*Carica papaya*), neem (*Azadirachta indica*), and Ashanti Blood (*Mussaenda erythrophylla*) are shown in Figure 1. Spectra are reported in the most informative region 1800–600 cm1 and 3000-2500. (Das et al., 2024)

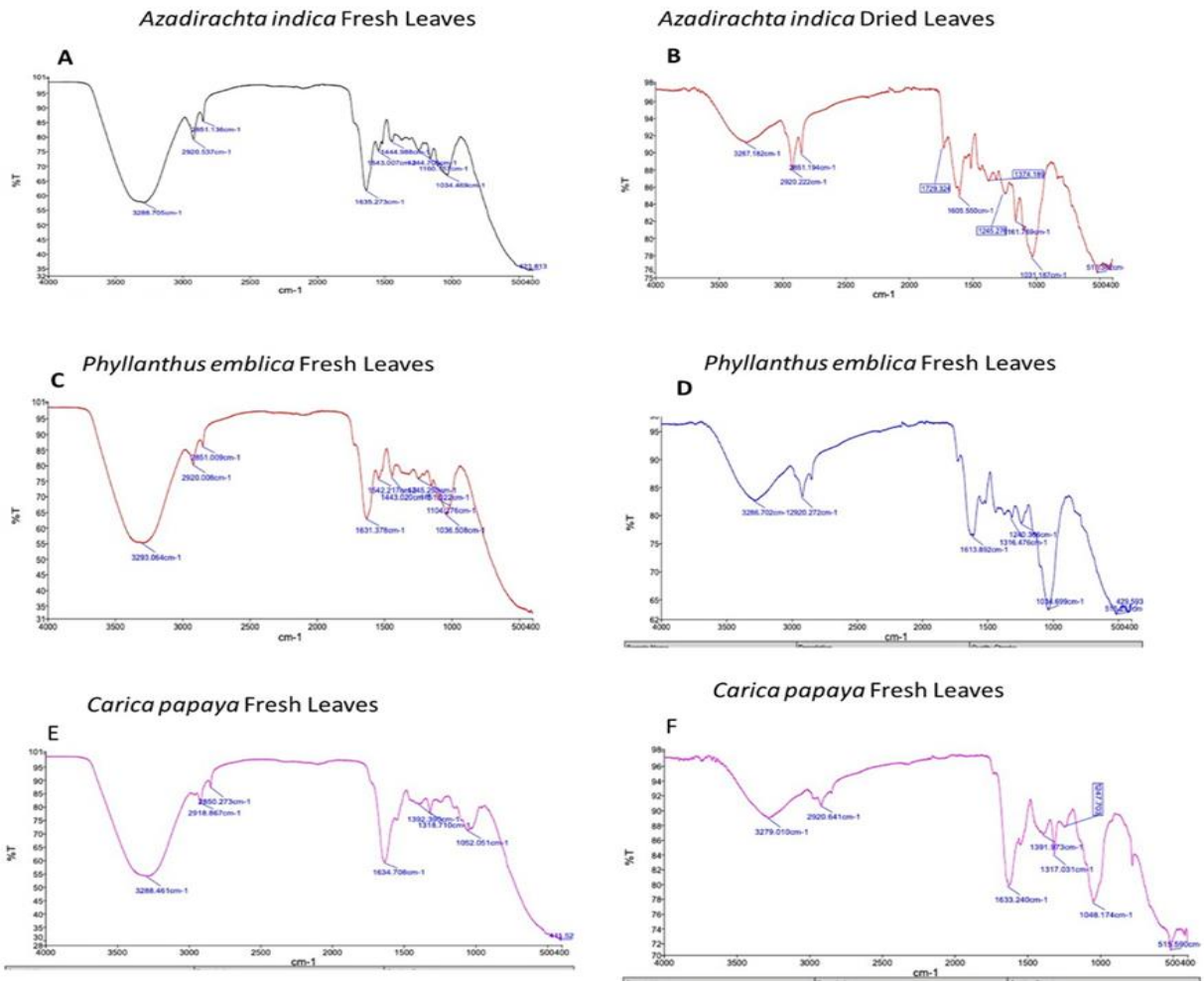

Fig. 1. ATR-FTIR spectra of fresh and dried leaves of *Azadirachta indica*, *Phyllanthus emblica*, and *Carica papaya* (A–F). Spectra were recorded across the 4000–400 cm^{-1} range, and comparative analysis highlights distinct differences in functional group profiles between fresh and dried samples

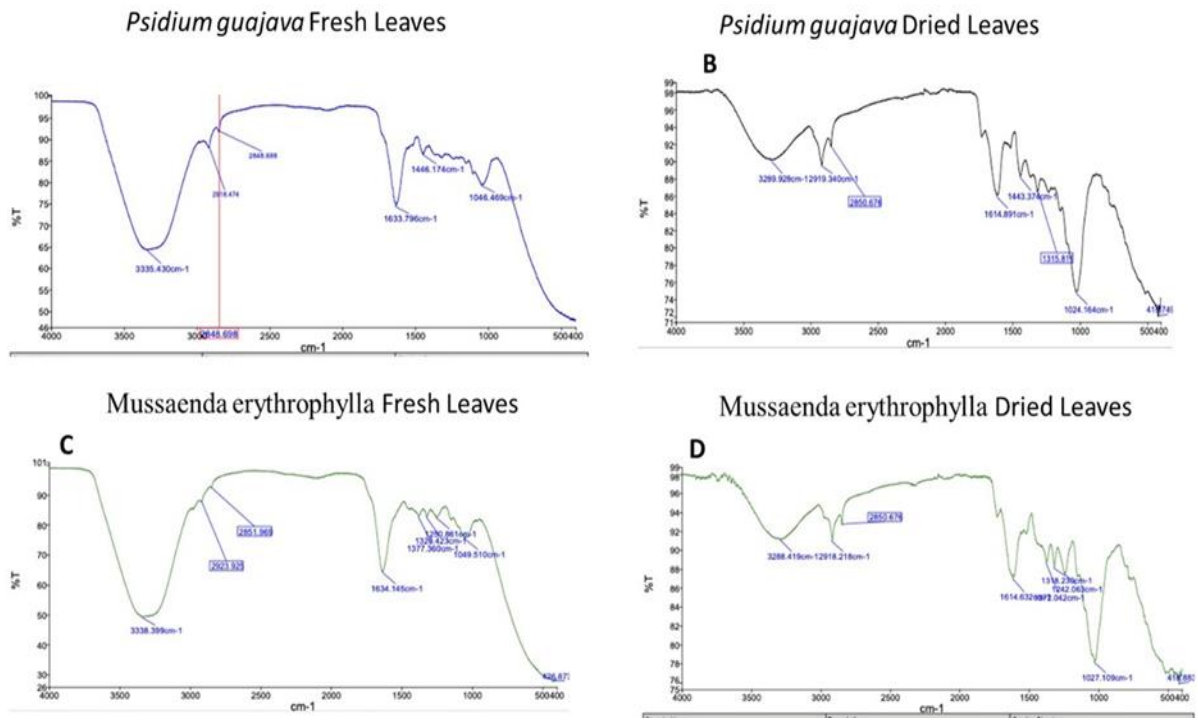

Fig. 2. ATR-FTIR spectra of fresh and dried leaves of *Psidium guajava* and *Mussaenda erythrophylla* (A–D). Spectra were recorded across the 4000–400 cm^{-1} range, and comparative analysis shows clear differences in the functional group profiles between fresh and dried samples

The dominant peak in the region between 3000 to 3500 in fresh leaves corresponds to the water content and after drying the dominant peak became week indicating water content from the leaves of the plant disappeared. The major and dominant peaks in all the leaves of plants Guava, Amla, Ashanti Blood, Neem and Pappaya are in the region 3000-2000 cm-1 assigned to lipids, 1800-1500 cm-1 for proteins, 1500-1200 for carbohydrates, and 1000-6000 for cell wall components and these peaks became dominant after drying. The region between 1000 and 1100 cm-1 is also called the fingerprint of the plant and corresponds to the cellulose content in leaves. The spectral profiles of leaves from all the plants are very similar to each other, even if slight differences concerning peaks intensities can be noted (Wilson et al., 2000; Canteri et al., 2019).

Among the plants examined, the protein-associated absorption band in the 1600–1650 cm^{-1} region was highest in the show flower, followed by guava, neem, papaya, and amla. Similarly, the cell wall– and chlorophyll-related region (1000–1050 cm^{-1}) showed stronger signals in neem, papaya, shoe flower, guava, and amla. These differences highlight the biochemical diversity and variation in molecular composition across the studied species. The peaks between 2900-2800 corresponds to the presence of alkanes C-H stretching. (Kancherla et al., 2025) (Ayvaz & Temizkan, 2018)

Across the plants analyzed, distinct spectral features were observed in all major functional group regions. In the lipid region (3000–2000 cm^{-1}), we detected characteristic O–H stretching vibrations associated with alcohols and carboxylic acids, N–H stretching from amides and amines, C–H stretching corresponding to benzene rings, alkynes, and alkenes, as well as aliphatic C–H stretching typical of alkanes. Signals corresponding to P–H stretching (phosphines) were also present (Nandiyanto et al., 2019). In the protein region (1800–1500 cm^{-1}), the spectra showed prominent C=O stretching bands indicative of ketones, along with C=C stretching associated with aromatic (benzene) structures. Additional peaks representing

N–H bending (nitro compounds) and C–O stretching (amides and ketones) further confirmed protein-related vibrational modes (Ji et al., 2020).

The carbohydrate region (1600–1200 cm^{-1}) displayed N=O stretching (nitro compounds), C–O–H bending characteristic of aldehydes, C–N stretching from amines, and C–O stretching vibrations representing esters, ethers, and alcohols. These features highlight the diversity of carbohydrate-associated functional groups present in the plant samples (Ji et al., 2020). In the cell wall component and chlorophyll region (1000–600 cm^{-1}), we observed S=O stretching (sulfoxides), recurrent C–N stretching peaks (amines), C–O stretching from alcohols, =C–H bending from aromatic (benzene) rings, and C–Cl stretching representing chlorides. Together, these signatures confirm the presence of structurally complex cell wall polymers and pigment-related compounds across the studied plants (Umar et al., 2023; Pan et al., 2007).

Conclusion

This study aimed to profile the chemical fingerprint of plant leaves using ATR-FTIR spectroscopy. We compared the functional group composition before and after drying the leaf samples to assess changes in biomolecular signatures. The results indicate that the plants are rich in polyphenols, lignin's, proteins, carbohydrates, and phosphates. This work provides a foundation for further research on the phytochemical composition and biological activities of medicinal plants. Fourier Transform Infrared (FTIR) spectroscopy has proven to be a reliable and sensitive technique for detecting the biomolecular composition of cells. In this study, we demonstrated the potential of ATR-FTIR spectroscopy for the rapid and reliable discrimination and identification of functional groups associated with the medicinal properties of both fresh and dried leaves. Our findings indicate that dried leaf samples provide clearer and more consistent spectral profiles, making them more suitable for further phytochemical and biomolecular analyses. We therefore recommend drying leaf samples prior to FTIR-based investigations to minimize moisture-related interference and to ensure more accurate assessment of biomolecule concentrations. The spectral region between 4000 and 400 cm^{-1} is particularly informative, as it provides a unique molecular fingerprint that enables reliable differentiation among plant species based on their biomolecular constituents.

References

Ayvaz, H., & Temizkan, R. (2018). Quick vacuum drying of liquid samples prior to ATR-FTIR spectral collection improves the quantitative prediction: a case study of milk adulteration. *International Journal of Food Science and Technology, 53*(11), 2482–2489. https://doi.org/10.1111/ijfs.13839

Aziza, A. E., Quezada, N., & Cherian, G. (2010). Feeding Camelina sativa meal to meat-type chickens: Effect on production performance and tissue fatty acid composition. *Journal of Applied Poultry Research, 19*(2), 157–168. https://doi.org/10.3382/japr.2009-00100

Blonk, B., & Cock, I. E. (2019). Interactive antimicrobial and toxicity profiles of Pittosporum angustifolium Lodd. extracts with conventional antimicrobials. *Journal of Integrative Medicine, 17*(4), 261–272. https://doi.org/10.1016/j.joim.2019.03.006

Cai, Y., Luo, Q., Sun, M., & Corke, H. (2004). Antioxidant activity and phenolic compounds of 112 traditional Chinese medicinal plants associated with anticancer. *Life Sciences, 74*(17), 2157–2184. https://doi.org/10.1016/j.lfs.2003.09.047

Canteri, M. H. G., Renard, C. M. G. C., Le Bourvellec, C., & Bureau, S. (2019). ATR-FTIR spectroscopy to determine cell wall composition: Application on a large diversity of fruits

and vegetables. *Carbohydrate Polymers, 212*, 186–196. https://doi.org/10.1016/j.carbpol.2019.02.021

Dal Bosco, A., Mattioli, S., Matics, Z., Szendrő, Z., Gerencsér, Z., Mancinelli, A. C., Kovács, M., Cullere, M., Castellini, C., & Dalle Zotte, A. (2019). *The antioxidant effectiveness of liquorice (Glycyrrhiza glabra L.) extract administered as dietary supplementation and/or as a burger additive in rabbit meat. Meat Science, 158*. https://doi.org/10.1016/j.meatsci.2019.107921

Das, S., Bhati, V., Dewangan, B. P., Gangal, A., Mishra, G. P., Dikshit, H. K., & Pawar, P. A. M. (2024). Combining Fourier-transform infrared spectroscopy and multivariate analysis for chemotyping of cell wall composition in Mungbean (Vigna radiata (L.) Wizcek). *Plant Methods, 20*(1). https://doi.org/10.1186/s13007-024-01260-w

Fu, Y., Luo, J., Qin, J., & Yang, M. (2019). Screening techniques for the identification of bioactive compounds in natural products. *Journal of Pharmaceutical and Biomedical Analysis*, *168*, 189-200. https://doi.org/10.1016/j.jpba.2019.02.027

Ji, Y., Yang, X., Ji, Z., Zhu, L., Ma, N., Chen, D., Jia, X., Tang, J., & Cao, Y. (2020). DFT-Calculated IR Spectrum Amide I, II, and III Band Contributions of N-Methylacetamide Fine Components. *ACS Omega, 5*(15), 8572–8578. https://doi.org/10.1021/acsomega.9b04421

Kancherla, M., Mary Shamya, A., Wasim Akram, S. A., John Christopher, J., Zuha Umme Kulsum, S., Athar Parvez, A., Begum, T., Kabiruddin Ahmed, K., Ahmed, N. Z., Meena, R., & Kumar, P. (2025). Phytochemical fingerprinting of ethanolic extract of Iṭrīfal Ṣaghīr – An unani formulation: standardization, HPTLC and GC–MS based analysis. *Results in Chemistry, 18.* https://doi.org/10.1016/j.rechem.2025.102824

Kumar, J. K., & Prasad, A. D. (2011). Identification and comparison of biomolecules in medicinal plants of Tephrosia tinctoria and Atylosia albicans by using FTIR. *Romanian Journal of Biophysics*, *21*(1), 63-71.

Lee, S. E., Hwang, H. J., Ha, J. S., Jeong, H. S., & Kim, J. H. (2003). Screening of medicinal plant extracts for antioxidant activity. *Life Sciences, 73*(2), 167–179. https://doi.org/10.1016/S0024-3205(03)00259-5

Lowe, H., Steele, B., Bryant, J., Fouad, E., Toyang, N., & Ngwa, W. (2021). Antiviral activity of Jamaican medicinal plants and isolated bioactive compounds. *Molecules*, *26*(3), 607. https://doi.org/10.3390/molecules26030607

Maaloul, S., Mahmoudi, M., Mighri, H., Ghzaiel, I., Bouhamda, T., Boughalleb, F., El Midaoui, A., Vejux, A., Lizard, G., & Abdellaoui, R. (2024). Tunisian Silybum Species: Important Sources of Polyphenols, Organic Acids, Minerals, and Proteins across Various Plant Organs. *Plants, 13*(7). https://doi.org/10.3390/plants13070989

Mandrone, M., Bonvicini, F., Lianza, M., Sanna, C., Maxia, A., Gentilomi, G. A., & Poli, F. (2019). Sardinian plants with antimicrobial potential. Biological screening with multivariate data treatment of thirty-six extracts. *Industrial Crops and Products, 137*, 557–565. https://doi.org/10.1016/j.indcrop.2019.05.069

Moussaoui, F., & Alaoui, T. (2016). Evaluation of antibacterial activity and synergistic effect between antibiotic and the essential oils of some medicinal plants. *Asian pacific journal of tropical biomedicine*, *6*(1), 32-37. https://doi.org/10.1016/j.apjtb.2015.09.024

Nandiyanto, A. B. D., Oktiani, R., & Ragadhita, R. (2019). How to read and interpret ftir spectroscope of organic material. *Indonesian Journal of Science and Technology, 4*(1), 97–118. https://doi.org/10.17509/ijost.v4i1.15806

Nikalje, G. C., Kumar, J., Nikam, T. D., & Suprasanna, P. (2019). FT-IR profiling reveals differential response of roots and leaves to salt stress in a halophyte Sesuvium portulacastrum (L.) L. *Biotechnology Reports, 23*. https://doi.org/10.1016/j.btre.2019.e00352

Pan, G., Du, Z., Zhang, C., Li, C., Yang, X., & Li, H. (2007). Effect of structure of bridging group on curing and properties of bisphenol-a based novolac epoxy resins. Polymer Journal, 39(5), 478–487. https://doi.org/10.1295/polymj.PJ2006201

Shahidi, F., & Ambigaipalan, P. (2015). Phenolics and polyphenolics in foods, beverages and spices: Antioxidant activity and health effects–A review. *Journal of functional foods*, *18*, 820-897. https://doi.org/10.1016/j.jff.2015.06.018

Subash, S., Braidy, N., Essa, M. M., Zayana, A. B., Ragini, V., Al-Adawi, S., Al-Asmi, A., & Guillemin, G. J. (2015). Long-term (15mo) dietary supplementation with pomegranates from Oman attenuates cognitive and behavioral deficits in a transgenic mice model of Alzheimer's disease. *Nutrition, 31*(1), 223–229. https://doi.org/10.1016/j.nut.2014.06.004

Süntar, I. (2020). Importance of ethnopharmacological studies in drug discovery: role of medicinal plants. *Phytochemistry Reviews*, *19*(5), 1199-1209. https://doi.org/10.1007/s11101-019-09629-9

Sytar, O., Hemmerich, I., Zivcak, M., Rauh, C., & Brestic, M. (2018). Comparative analysis of bioactive phenolic compounds composition from 26 medicinal plants. *Saudi Journal of Biological Sciences, 25*(4), 631–641. https://doi.org/10.1016/j.sjbs.2016.01.036

Tran, N., Pham, B., & Le, L. (2020). Bioactive compounds in anti-diabetic plants: From herbal medicine to modern drug discovery. *Biology*, *9*(9), 252. https://doi.org/10.3390/biology9090252

Umar, A. H., Syahruni, R., Ranteta'dung, I., & Rafi, M. (2023). FTIR-based fingerprinting combined with chemometrics method for rapid discrimination of Jatropha spp. (Euphorbiaceae) from different regions in South Sulawesi. *Journal of Applied Pharmaceutical Science, 13*(1), 139–149. https://doi.org/10.7324/JAPS.2023.130113

Walters, N. A., de Beer, D., de Villiers, A., Walczak, B., & Joubert, E. (2019). Genotypic variation in phenolic composition of Cyclopia pubescens (honeybush tea) seedling plants. Journal of Food Composition and Analysis, 78, 129–137. https://doi.org/10.1016/j.jfca.2019.02.006

Wilson, R. H., Smith, A. C., Kacuráková, M., Saunders, P. K., Wellner, N., & Waldron, K. W. (2000). The mechanical properties and molecular dynamics of plant cell wall polysaccharides studied by Fourier-transform infrared spectroscopy. *Plant Physiology*, *124*(1), 397-406.

Xiong, Y., & Long, C. (2020). An ethnoveterinary study on medicinal plants used by the Buyi people in Southwest Guizhou, China. *Journal of ethnobiology and ethnomedicine*, *16*(1), 46. https://doi.org/10.1186/s13002-020-00396-y

Zengin, G., Ceylan, R., Katanić, J., Aktumsek, A., Matić, S., Boroja, T., ... & Mahomoodally, M. F. (2018). Exploring the therapeutic potential and phenolic composition of two

Turkish ethnomedicinal plants–Ajuga orientalis L. and Arnebia densiflora (Nordm.) Ledeb. *Industrial Crops and Products*, *116*, 240-248. https://doi.org/10.1016/j.indcrop.2018.02.054